Optics Letters

Optically isotropic, electrically tunable liquid crystal droplet arrays formed by photopolymerization-induced phase separation

HAITAO DAI,[1,*] LIN CHEN,[1] BIN ZHANG,[1] GUANGYUAN SI,[2] AND YAN JUN LIU[3,4]

[1]Tianjin Key Laboratory of Low Dimensional Materials Physics and Preparing Technology, School of Science, Tianjin University, Tianjin 300072, China
[2]College of Information Science and Engineering, Northeastern University, Shenyang 110004, China
[3]Institute of Materials Research and Engineering, Agency for Science, Technology and Research (A*STAR), 3 Research Link, Singapore 117602, Singapore
[4]e-mail: liuy@imre.a-star.edu.sg
*Corresponding author: htdai@tju.edu.cn

Received 30 March 2015; revised 19 May 2015; accepted 19 May 2015; posted 21 May 2015 (Doc. ID 237150); published 4 June 2015

Phase separation has been an interesting and important topic in liquid crystal (LC)–polymer composites. We investigated the photopolymerization-induced phase separation in an LC–polymer composite through a maskless lithographic system based on an amplitude-modulated spatial light modulator. By optimizing both exposure conditions and materials, we achieved a two-dimensional (2D) liquid crystal droplet array (LCDA) in the LC–polymer composite. Further investigations revealed that such 2D LCDAs, working as microlens arrays, demonstrated polarization-independent, electrically tunable focusing properties under a certain voltage. With advantages in cost-effectiveness, fast fabrication, and polarization-independent, electrically tunable focusing, such phase-separated microlens arrays in the LC–polymer composite could find many potential optical applications. © 2015 Optical Society of America

OCIS codes: (090.1970) Diffractive optics; (130.0250) Optoelectronics; (230.3720) Liquid-crystal devices.

http://dx.doi.org/10.1364/OL.40.002723

Liquid crystal (LC)-polymer composite materials are an attractive electro-optical medium, which has been extensively explored for a wide range of applications [1–3]. Thus far, researchers have developed different LC–polymer composite systems [4–6]. In these material systems, LC molecules are dispersed in the polymer matrix via photopolymerization-induced phase separation. By controlling the phase separation, it gives additional freedom to construct electric-optical devices with specific functions [7–9]. A big advantage for LC–polymer composites is that the relaxation time of LC molecules can be effectively decreased due to strong anchoring strength of the polymer matrix on LC molecules [10]. However, the strong anchoring strength will also lead to a high driving voltage, making the composites vulnerable to the driving voltage [11]. Therefore, a trade-off between the response time and the driving voltage has to be made depending on applications. In comparison to the structure of micro-/nano-LC droplets encapsulated in a polymer matrix, mesoscale LC content formed via relatively complete phase separation in LC–polymer composites [12] presents excellent electro-optical response, such as low driving voltage and high diffraction efficiency. Nowadays, many optical devices have been developed based on mesoscale photopolymerization-induced phase separation [13–15].

To achieve LC/polymer devices with desired functions, phase separation plays a crucial role since it determines the LC distribution as well as alignment. For photopolymerization-induced phase separation, LC distribution and alignment depend largely on the exposure pattern, intensity, time, and temperature. Generally, a mask is used to achieve the designed exposure pattern. This method, however, is limited by the fixed mask [16]. Recently, a maskless technique based on a spatial light modulator (SLM) has been widely adopted in micro-/nano-structures fabrication with advantages of programmable capability and low cost [13,17].

In this Letter, we report on a two-dimensional (2D) LC droplet array (LCDA) formed by photopolymerization-induced phase separation in an LC–polymer composite. The photopolymerization-induced phase separation is carried out using a maskless lithographic system based on an amplitude-modulated spatial light modulator (a-SLM). Such 2D LCDAs can work as microlens arrays since they demonstrate polarization-independent, electrically tunable focusing properties under a certain voltage. This kind microlens array may find many photonic applications that require polarization-insensitive operation.

The initial syrup for the LC–polymer composite is composed of a photoinitiator, Rose Bengal (RB), co-initiator, *N*-phenylglycine (NPG), cross-linking monomer, *N*-vinyl-2-pyrrolidone (NVP), Norland optical adhesive, NOA 61, and nematic LC E48 ($TN_1 = 58°C$, $\Delta n = n_e - n_o = 0.23$, $\Delta\varepsilon = 43$) with the ratio of 1:1:6:62:30 by weight. After

being fully blended in an ultrasonic tank for about 1.5 h, the syrup was capillary filled into an empty LC cell (assembled with two pieces of indium-tin-oxide glass separated by a 20 μm spacer and sealed by epoxy resins).

The prepared LC cell was then exposed to the patterned light illumination, which was created by modulating a collimated light beam via the a-SLM. The experimental setup is shown in Fig. 1. The light from a laser (Verdi V2, wavelength: 532 nm) was first collimated and then modulated by the a-SLM (pixel size: 10.8 × 10.8 μm). The modulated light pattern was then transcribed into the LC–polymer composite via photopolymerization-induced phase separation. A CMOS camera (Thorlabs DCC1645C) was used to monitor the formed patterns by a-SLM. The optimized exposure intensity was 2.5 mW/cm^2 and the exposure time was about 20 min at room temperature. After exposure, the LC cell was further cured by a UV light source for 10 min to ensure the complete polymerization. In our experiments, a square lattice was used to prepare the 2D LCDA, as shown in Fig. 1. The lattice constant was about 86.4 μm, and the binary pattern was transcribed equally to the sample by an achromatic doublet with $f = 15$ cm.

The morphology of the formed 2D LCDA pattern was first observed under a polarized optical microscope (POM) (Olympus IX 71). Figure 2(a) shows the recorded images of the LCDA in a wide view under POM. Figures 2(b) and 2(c) show the enlarged images without polarizers and with crossed polarizers, respectively. It is obvious that large LC droplets are formed within the polymer matrix, indicating successful photopolymerization-induced phase separation between LCs and polymers. The formed LC droplets have an average diameter of about 89.7 μm, which is slightly larger than the lattice period due to the misalignment of the imaging system and diffraction. A closer look at the morphology under POM [Fig. 2(c)] shows that a speckle-like background exists around LC droplets, implying that some LC molecules are still trapped in the polymer matrix. More importantly, the LC droplets observed under POM demonstrate quite different conoscopic interference textures, which means the LC molecules are aligned differently

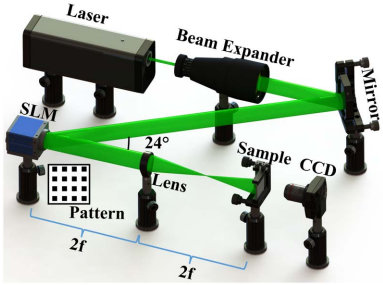

Fig. 1. Schematic of the experimental setup.

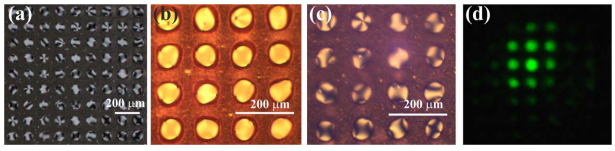

Fig. 2. (a) Wide view morphology of the 2D LCDAs observed under POM. Magnified views (b) without polarizers and (c) with crossed polarizers. (d) Diffraction pattern of the sample.

inside each droplet due to random anchoring direction caused by the polymer walls. As known, different alignments will result in nonuniform electro-optic behaviors. Further investigations are still ongoing with the aim to achieve the same LC alignment inside each droplet. Figure 2(d) shows the diffraction pattern of the 2D LCDA structure, which further verifies the square lattice shape of the fabricated sample.

It is worth mentioning that compared to the designed square pattern, the LC droplets show a round shape in the top-view due to the diffraction of incident light. As a result, cylindrical-like LC droplets are formed in our experiment considering the low aspect ratio of diameter (89.7 μm) versus height (20 μm). To have better or even exact pattern transfer, utilizing incoherent light could be a better option.

We further investigated the electro-optical properties of the 2D LCDA by illuminating a collimated laser beam (beam size: ~2 cm in diameter, laser wavelength: 532 nm) under different driving voltages. The transmitted intensity distribution was recorded by the CMOS camera equipped with a 10× objective. Figure 3 shows the electro-optical results recorded when the driving voltage varies from 0 to 25 V with a 5 V interval. Some nonuniform focal points were first observed in Fig. 3(a) with zero voltage. As the driving voltage increases up to 5 V, the nonuniform focal points disappear, as shown in Fig. 3(b). As the driving voltage further increases to about 10 V, weak and uniform focal points appear, as shown in Fig. 3(c). The focal points become clearer and stronger by further increasing the driving voltage, as shown in Figs. 3(d)–3(f). Note that the focal points disappeared at about 4 V and reappeared at 6.5 V (defined as the threshold, E_{th}) in our experiments. The polarized directions of incident beams are also set as horizontal, as shown in Fig. 3(a).

The observed focusing effects in Fig. 3 can be understood with the alignment and realignment of LC molecules inside the droplets. The top row in Fig. 4 schematically illustrates the working principle of our 2D LCDA. When there is no applied voltage, random alignment of LC molecules inside each cylindrical-like droplet is presented subject to the anchoring strength of polymer walls, as shown in Fig. 4(a). The boundaries between LC regions and polymer walls are gradient due to the disordered alignment of LC molecules near polymer walls. Moreover, the random alignment of LC molecules varies from each individual droplet. Therefore, we observed nonuniform focusing points [Fig. 3(a)]. Near the threshold voltage, the director of LC molecules inside the droplets will be disturbed and

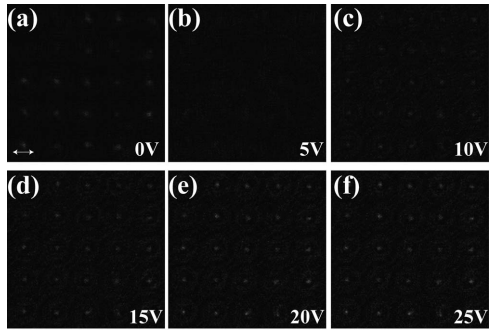

Fig. 3. Intensity distribution in the focal plane recorded by the CCD when (a) 0 V, (b) 5 V, (c) 10 V, (d) 15 V, (e) 20 V, and (f) 25 V voltages were applied.

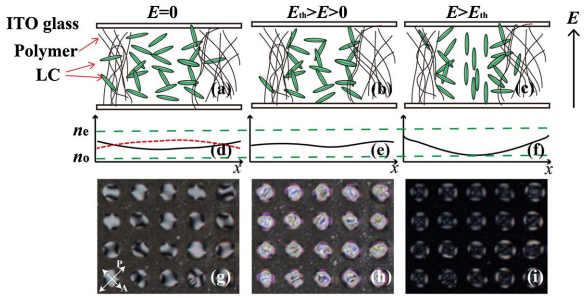

Fig. 4. Schematic of the LC molecules (top row), schematic of the index profiles (middle row), and the observed POM images (bottom row) for the cylindrical-like droplets with three typical operation ranges: $E = 0$, $E_{th} > E > 0$, and $E > E_{th}$.

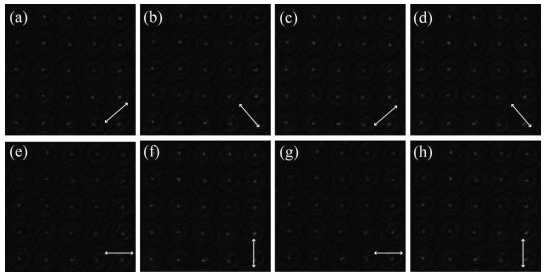

Fig. 5. Intensity of the focusing points of 2D LCDAs under illuminating light with different polarizations and different driving voltages of (a) 45°, 20 V; (b) 135°, 20 V; (c) 45°, 50 V; (d) 135°, 50 V; (e) 0°, 20 V; (f) 90°, 20 V; (g) 0°, 50 V; and (h) 90°, 50 V.

more disordered alignment of LC molecules is formed, as shown in Fig. 4(b), which corresponds to a more uniform illumination on the imaging plane. Therefore, no focusing effect was observed. When a larger voltage is applied, LC molecules around the medial axis of the droplet will start to align along the external electric field direction. However, due to the strong anchoring strength of the polymer wall, LC molecules near the polymer wall will still keep original alignment, as shown in Fig. 4(c). Since the external electric field and light propagation have the same direction, the incident light will experience the ordinary index (n_o) regardless of light polarizations for the medial part LCs. While for the marginal part LCs near the polymer walls, the effective index experienced by the incident light is determined by the angle (θ) between the LC director and the polarization direction of incident light, which is written as $n_{\text{eff}}(\theta) = [\cos^2(\theta)/n_o^2 + \sin^2(\theta)/n_e^2]^{-1/2}$. This effective index is larger than n_o for a positive LC (e.g., E48), or equal in the case of $\theta = 0°$. As a result, the LC droplet has a concave refractive index profile and focal points are hence formed, as shown in Fig. 3(c). When the voltage further increases, more and more LC molecules will align along the electric field direction, inducing a clearer index profile and subsequently a stronger focusing effect. One has to note that the orientation of LC molecules contacting polymer walls cannot be tuned with even larger voltage due to the strong anchoring energy. Therefore, the focal points still exist even with 50 V applied voltage.

The middle row in Fig. 4 shows the schematically described index profiles corresponding to the cases in Fig. 4(a)–4(c). The solid and dotted lines correspond to different configurations of LC droplets without applied voltages. The bottom row in Fig. 4 shows the images observed under POM with various voltages, which can clearly verify the transformation of LC alignment as discussed above. When there is no applied voltage, the texture of conoscopic interference in the LC droplets proves individual aligning manners of LC molecules, which correspond to the nonuniform distribution of focal points [Fig. 4(g)]. With an increase in the applied voltage ($< E_{th}$), the uniform brightness in the droplets depicts chaos alignment of the LC in the droplets [Fig. 4(h)]. However, when the driving voltage is high enough, four bright lobes at the edge and a dark center in each LC droplet are clearly observed [Fig. 4(i)]. The secondary lobes, closer to the middle of the droplet, were observed in Fig. 4(i) as well. This observation is ascribed to the conoscopic interference of a uniaxial crystal with its optical axis perpendicular to surface, which correspond to the center area in each individual droplet where the LC molecules are aligned along with the electric field direction under a sufficient voltage, as shown in Fig. 4(c). The configurations of the polarizer (P) and the analyzer (A) in Figs. 4(g)–4(i) are the same as the labeled cross arrows in Fig. 4(g).

In general, most LC lenses show polarization-dependent focusing due to birefringence. In our experiment, different polarized beams are impinged onto our 2D LCDAs to check the focusing property. Figures 5(a)–5(h) depict the intensity distribution on the focal plane with different polarizations and voltages. The results confirm that focal points of our 2D LCDAs are polarization-independent with the applied voltage above the threshold. The focal points keep unchanged when the polarization direction rotates from 0° to 180°. This property is ascribed to the unique LC alignment inside the droplets as we discussed.

Due to the large LC droplets, the relaxation time of LC droplets array is about 0.24 s. Generally, the switch-on time is related to the applied voltage, for our device, the on-time is about 30 ms covering the stages of focal point disappearance and regeneration when driven by a modulated square wave (1 kHz square wave modulated by a 1.5 Hz square wave) with an amplitude of 13 Vpp.

In conclusion, we have demonstrated 2D LCDA via the photopolymerization-induced phase separation in an LC–polymer composite using a maskless lithography technique. Clear phase separation between the LC and the polymer has been achieved. The 2D LCDA patterns can also work as microlens arrays since they demonstrated an obvious focusing effect. In addition, the focusing is optically isotropic (i.e., polarization-independent) at applied voltages far above the threshold. With advantages in cost-effectiveness, fast fabrication, and polarization-independent, electrically tunable focusing, such phase-separated microlens arrays in the LC–polymer composite could find many potential optical applications.

Key project of Nature Science Foundation of Tianjin (14JCZDJC31400); National Natural Science Foundation of China (NSFC) (11204208, 61177061); Open Research Fund of the State Key Laboratory of Transient Optics and Photonics (Chinese Academy of Sciences).

REFERENCES

1. V. P. Tondiglia, L. V. Natarajan, R. L. Sutherland, D. Tomlin, and T. J. Bunning, Adv. Mater. **14**, 187 (2002).

2. H. T. Dai, Y. J. Liu, X. W. Sun, and D. Luo, Opt. Express **17**, 4317 (2009).
3. L. V. Natarajan, C. K. Shepherd, D. M. Brandelik, R. L. Sutherland, S. Chandra, V. P. Tondiglia, D. Tomlin, and T. J. Bunning, Chem. Mater. **15**, 2477 (2003).
4. D. C. Jung, S. L. Sang, C. P. Su, B. K. Yang, and W. H. Jin, J. Appl. Poly. Sci. **130**, 3098 (2013).
5. C. Y. Li and T. J. Bunning, Curr. Opin. Chem. Eng. **2**, 63 (2013).
6. C. V. Rajaram and S. D. Hudson, Chem. Mater. **7**, 2300 (1995).
7. H. T. Dai, X. W. Sun, D. Luo, and Y. J. Liu, Opt. Express **17**, 19365 (2009).
8. H. W. Ren, S. Xu, and S. T. Wu, Opt. Express **20**, 26464 (2012).
9. Y. H. Lin, H. W. Ren, Y. H. Wu, S. T. Wu, Y. Zhao, J. Y. Fang, and H. C. Lin, Opt. Express **16**, 17591 (2008).
10. T. J. Bunning, L. V. Natarajan, V. P. Tondiglia, and R. L. Sutherland, Ann. Rev. Mater. Sci. **30**, 83 (2000).
11. A. Marino, F. Vita, V. Tkachhenko, R. Caputo, C. Umeton, A. Veltri, and G. Abbate, Euro. Phys. J. E **15**, 47 (2004).
12. R. Caputo, L. D. Sio, A. Veltri, and C. Umeton, Opt. Lett. **29**, 1261 (2004).
13. M. Infusino, A. D. Luca, V. Barna, R. Caputo, and C. Umeton, Opt. Express **20**, 23138 (2012).
14. L. D. Sio, N. Tabiryan, and T. Bunning, Appl. Phys. Lett. **104**, 221112 (2014).
15. D. Alj, R. Caputo, and C. Umeton, Opt. Lett. **39**, 6201 (2014).
16. Y. J. Liu and X. W. Sun, Appl. Phys. Lett. **90**, 191118 (2007).
17. R. K. Kwang, Y. Junsin, H. C. Sung, H. K. Nam, W. C. Myung, S. S. Bo, and C. Byoungdeog, Appl. Surf. Sci. **255**, 7835 (2009).